AD_____
(Leave blank)

Award Number:
W81XWH-08-1-0543

TITLE:
Targeted CNx Nanowire-Drug Complexes for enhanced Chemotherapeutic Efficacy

PRINCIPAL INVESTIGATOR:
David Carroll PhD.

CONTRACTING ORGANIZATION:
Wake Forest University
Winston-Salem NC 27109

REPORT DATE:
September 2009

TYPE OF REPORT:
Annual

PREPARED FOR: U.S. Army Medical Research and Materiel Command
Fort Detrick, Maryland 21702-5012

DISTRIBUTION STATEMENT: (Check one)

X Approved for public release; distribution unlimited

☐ Distribution limited to U.S. Government agencies only;
report contains proprietary information

REPORT DOCUMENTATION PAGE

Form Approved
OMB No. 0704-0188

1. REPORT DATE *(DD-MM-YYYY)*	**2. REPORT TYPE**	**3. DATES COVERED** *(From - To)*
01-Sep 2009	Annual	1SEP 2008 – 31 Aug 2009

4. TITLE AND SUBTITLE
Targeted CNx Nanowire-Drug Complexes for enhanced Chemotherapeutic Efficacy

5a. CONTRACT NUMBER
W81XWH-08-1-0543

5b. GRANT NUMBER

5c. PROGRAM ELEMENT NUMBER

6. AUTHOR(S)
David Carroll

Email: carroldl@wfu.edu

5d. PROJECT NUMBER

5e. TASK NUMBER

5f. WORK UNIT NUMBER

7. PERFORMING ORGANIZATION NAME(S) AND ADDRESS(ES)

Wake Forest University
Winston-Salem NC 27109

8. PERFORMING ORGANIZATION REPORT NUMBER 1

9. SPONSORING / MONITORING AGENCY NAME(S) AND ADDRESS(ES)
U.S. Army Medical Research and Materiel Command, Fort Detrick, Maryland 21702-5012

10. SPONSOR/MONITOR'S ACRONYM(S)

11. SPONSOR/MONITOR'S REPORT NUMBER(S)

12. DISTRIBUTION / AVAILABILITY STATEMENT

Approved for public release

13. SUPPLEMENTARY NOTES

14. ABSTRACT

Recently the use of carbon nanotubes (CNT), Ag nanoshells, and other Nanowires have been shown to be effective in photo-ablating cultured cells. In these early demonstrations, penetrating IR (~1.04 micron) generates heating in the nano-object to affect temperature rises in the surrounding cells. These promising approaches to therapeutic heat delivery is limited because unrealistically high radiation intensities (>100 mW) must be delivered at the dermis to provide the necessary heating for cell death deep in tissues. Further, these "nanocarriers" lack specificity or targeting modalities needed to achieve critical particle density for ideal heat transduction. Targeting moeties can be coupled to carbon nitride nanotube. The resulting conjugates can be activated to photo-ablate tumors with an extraordinarily small amount of power (< 10 mW at the tumor) while locally releasing chemotherapeutics that further enhance efficacy.

15. SUBJECT TERMS
None provided.

16. SECURITY CLASSIFICATION OF: U			**17. LIMITATION OF ABSTRACT**	**18. NUMBER OF PAGES**	**19a. NAME OF RESPONSIBLE PERSON**
a. REPORT	**b. ABSTRACT**	**c. THIS PAGE**	UU	21	USAMRMC
					19b. TELEPHONE NUMBER *(include area code)*

Final Report

Statement of work:

Task 1: *Development of Herceptin-CNWs in cell culture*:

a. Using our experience conjugation chemistries on fullerenes (Diels-Alder cycloaddition), we will construct CNW conjugates using CVD grown nanotubes and herceptin. (Months 1 – 4)
b. We will demonstrate that the conjugates' photo-ablative properties are significantly superior to intercellular forms of ablative therapeutics using *in situ* cell studies (cell lines listed below). (Month 5)

Task 2: Targeting and ablation of breast cancer cells in cell culture and mouse models, with the Herceptin- CNWs:

a. The interaction of the Herceptin-CNW conjugate will be tested in the immunoblotting and immunofluorescence experiments. We will employ HER-2 negative breast cancer cells (MCF-7 and MDA MB 231) and HER-2 positive cells (SK-Br-3 and BT474), and a Herceptin resistant BT474 cell line. (Month 6 – 8)
b. We will demonstrate that the conjugated nanotubes phototheramlly-ablate Herceptin positive breast cancer cells orthotopically implanted in athymic nude mice. (Month 9 – 10)
c. We will determine the optimized concentration of the conjugate for given depths within the mice. (Month 11-12)

Accomplishments:

To establish the feasibility of conferring aqueous solubility to MWNTs using DNA which could consequently be used in targeting, and to investigate to what extent DNA-encased MWNTs are useful for thermal ablation of malignant tissue. Multi-walled carbon nanotubes (MWNTs), strongly absorb near infrared (nIR) radiation and efficiently convert absorbed energy to released heat which can be used for localized hyperthermia applications. The relative efficiency of conversion of nIR irradiation into heat for DNA-encased MWNTs relative to non-DNA-encased MWNTs and other materials is an important consideration for identifying which type of nanomaterial is best-suited for *in vivo* thermal ablation approaches (Boldor et al., 2008). We have undertaken an analysis of the time-, power-, and concentration-dependence of heat generation from DNA-encased MWNTs. We demonstrate that DNA-encased MWNTs produce larger amounts of heat than non-DNA-encased MWNTs indicating that DNA-encasement may increase the utility of MWNTs for thermal ablative applications. Further, we demonstrate that DNA-encased MWNTs efficiently eradicate tumor xenografts *in vivo* in a mouse model of human cancer. Complete tumor eradication was achieved with a single treatment under conditions that resulted in no injury or damage to normal tissues. These finding demonstrate that DNA-encased MWNTs are useful for development of molecularly-targeted nanoparticles for selective thermal ablation of malignant tissue in humans.

We demonstrate that DNA-encasement efficiently solubilizes MWNTs and that DNA-encased MWNTs can be used to sensitize tumor tissue to nIR irradiation and used to completely eradicate a tumor mass. Heat is generated upon irradiation of DNA-encased MWNTs with a linear dependence on both laser power and time. A single treatment consisting of intratumoral injection of MWNTs (100 μl of a 500 μg/mL solution) followed by laser irradiation at 1064 nm, 2.5 W/cm^2 completely eradicated PC3 xenograft tumors in 8/8 (100%) of nu/nu mice. Control tumors that received only MWNT injection or laser irradiation showed tumor growth rates

indistinguishable from control tumors that received no treatment. Non-malignant tissues displayed no long term damage from treatment. The results demonstrate that DNA-encased MWNTs can be used effectively for selective thermal ablation for cancer treatment.

Report on *Task 1*: *Development of Herceptin-CNWs in cell culture*:

a. Using our experience conjugation chemistries on fullerenes (Diels-Alder cycloaddition), we will construct CNW conjugates using CVD grown nanotubes and herceptin. (Months 1 – 4)
b. We will demonstrate that the conjugates' photo-ablative properties are significantly superior to intercellular forms of ablative therapeutics using *in situ* cell studies (cell lines listed below). (Month 5)

Task1a.

Herceptin conjugated Nitrogen doped Multiwalled Carbon Nanotubes were created using standard Diels-Alder Chemistries. A wide variety of N-MWNTs were used for this but in all cases it was found that the adduct denatured around the nanotube forming crystalline formations. This resulted in nanotube-protein precipitates and insolubility. Possible ways around this included using longer tethers for the adduct. This was tried but coupling chemistries suffered from steric considerations for such large molecules.

After the first four months of this, we made the decision to move to a different targeting meaty, replacing herceptin with something else. Since the point of the experiment was to show that N-MWNTs could be targeted to tumor tissues or cell lines, use of another targeting species was deemed to not significantly alter the aims of the work and would provide for a faster route toward demonstrations in the time frames allotted. Our second approach was more successful, the use of aptamers.

Details of the successful approach to building N-MWNTs with targeting molecule:

Raw, carbon vapor deposition (CVD) MWNTs (0.05 mg/mL) were sonicated in a 4μM (0.05mg/mL) aqueous solution of single-stranded DNA (ssDNA; e.g. $d(GT)_{40}$) at 20 ^{o}C for 50 min using a bath sonicator to yield a solution of MWNTs non-covalently associated with ssDNA (DNA-encased MWNTs). The mixture was maintained at room temperature overnight followed by centrifugation at 2500 x g for 30 min to pellet MWNT aggregates and any insoluble material. The resulting translucent supernatant consisting of DNA-encased MWNTs was filtered through a 100-kDa molecular weight cutoff (MWCO) filters (Millipore) and extensively washed with 15 mL dH_2O to remove any unbound ssDNA. The filtration and washing steps were repeated 10 times and the efficiency of removal for free DNA was confirmed by no detectable absorbance of the final filtrates at 260 nm. The concentration of MWNT solution was determined by optical absorbance from a pre-established standard curve at 808 nm obtained using a DU800 UV-Vis spectrophotometer (Beckman Coulter). The fluorescently-labeled MWNT-DNA complex was prepared in an identical manner as for non-fluorescent complex except the ssDNA was fluorescently-labeled at the 5' terminus with FAM (Glenn Research).

We used Microscopic Characterization of Aptamer Functionalized N-MWNT to "see" our result.

AFM images were acquired under ambient conditions using a Nanoscope IIIA (Veeco Instruments, Plainview, NY) in tapping mode using silicon cantilevers (Nanosensor^{TM}, type PPP-NCLR-W, force constant k = 21-98 N/m, NanoAndMore, Lady's Island, SC). Surfaces for AFM imaging were prepared by depositing 50 mM $MgCl_2$ onto freshly cleaved ruby muscovite mica surface (Paramount

Corporation, NY) and allowed to dry in air. The mica surface was thoroughly rinsed with de-ionized water (Milli-Q Watersystem, Millipore Corp. Bedford, MA) to remove excess salt, and then dried using a gentle stream of Nitrogen gas. A 20 µL drop of DNA-MWNT solution (5 µg/mL) was deposited on the substrate and air-dried. The length and diameter of the tubes was analyzed using standard Nanoscope software (version 6.13).

For scanning electron microscopy (SEM), freshly cleaved mica was treated with 100 mM $MgCl_2$ and washed thoroughly with distilled water to remove excess salt. A 5µl drop of 25 µg/ml MWNT:DNA solution was then evenly dispersed on the mica surface and allowed to dry. The mica with dried MWNT:DNA complex was then pasted onto a stainless steel slab using silver paint. The mica surface on the slab was then sputter-coated with a very thin layer of gold-palladium mixture followed by drying. SEM images were obtained using a JEOL (JSM – 6330 F) field emission scanning electron microscope under a high vacuum conditions, using secondary electron emission mode at a working distance of 10 mm, a 12 µA probe current, and an accelerating voltage of 2.00 kV.

AFM and SEM images of DNA-encased MWNTs were obtained in order to assess to what extent aqueous solutions of DNA-encased MWNTs were mono-dispersed and to assess the range of MWNT size distributions in the DNA-encased samples. Fig. 1 shows a typical AFM image of a DNA-encased MWNT sample. It can be seen that the nanotubes are mostly well dispersed, with many single nanotubes and some small aggregates consisting of a few MWNTs each with clearly distinguishable nanotubes that touch each other. The presence of DNA is seen as a thickening of the MWNTs. The SEM images display comparable physical properties as those observed in the AFM images (Fig. 1). It can also be seen that the tubes have a range of lengths and diameters, and that most of them are curved. Continuous variations in NT curvature have been attributed to elasticity while bends in MWNT structures may be caused by topological defects (Han et al., 1998). Only a few globular features are visible. A more detailed analysis of nanotube morphology is shown in Fig. 1b-d. The nanotubes had an average diameter of 49 nm, an average length of 571 nm, and an average aspect ratio (length/diameter) of 13.

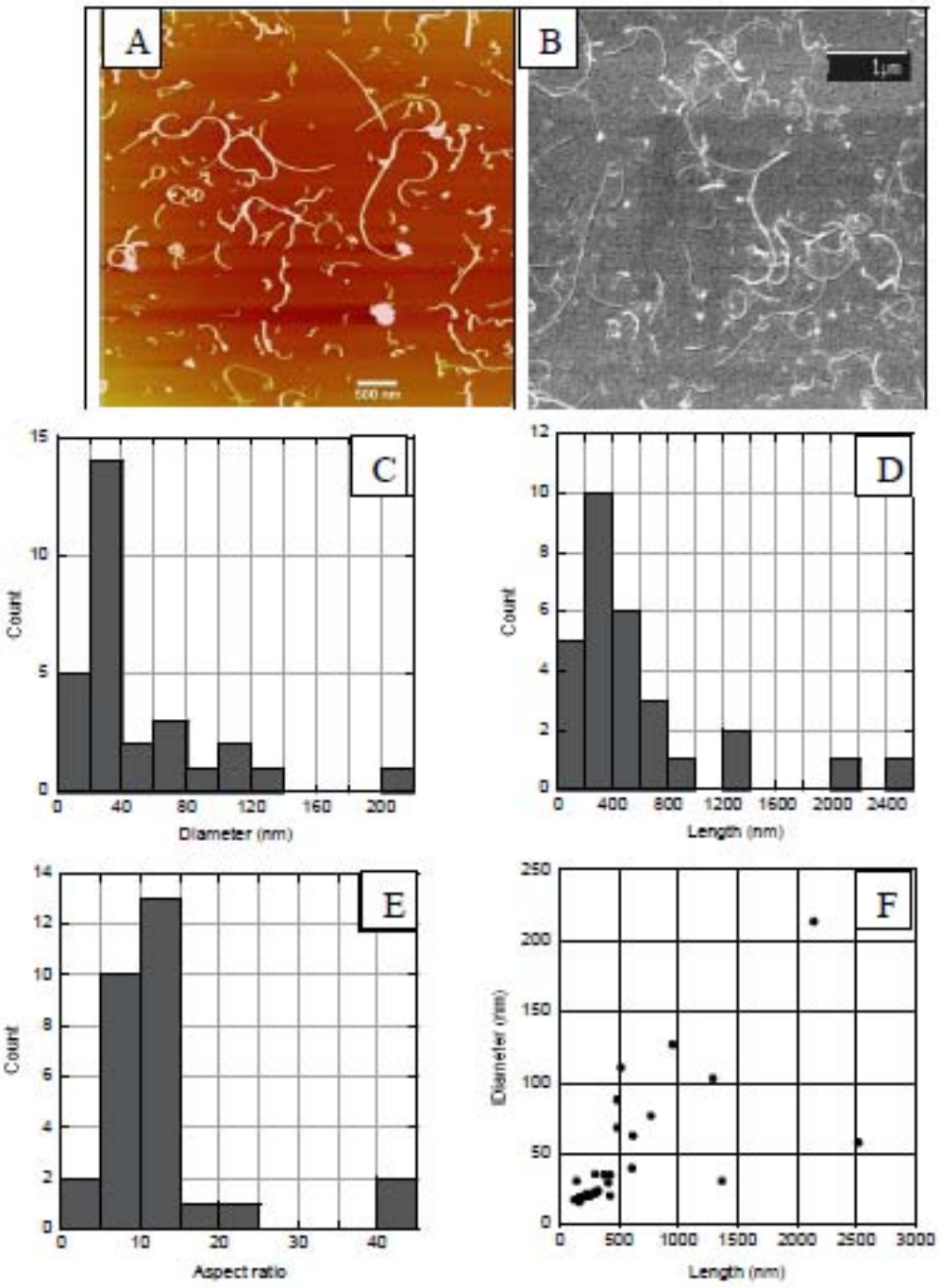

Figure 1: microanalysis of products

Spectroscopic Characterization of Aptamer functionalized N-MWNT:

DNA functionalized MWNTs were characterized by optical absorption spectroscopy and Raman spectroscopy. MWNTs solubilized with polyethylene glycol (PEG) were used as an aqueous-soluble control. Optical absorption spectra for the DNA-encased and PEG-solubilized MWNTs were obtained by using a dual-beam Perkin Elmer λ 19 UV-Vis-NIR spectrophotometer. The wavelength range 250 – 1400 nm was scanned at 2.5 nm/s.

Raman spectra were acquired using a Deltanu Advantage 532 Raman spectrometer. The region from 3400 – 200 cm^{-1} was scanned at 532 nm excitation. Raman spectra of non-DNA complexed MWNT was obtained by placing a dry powder sample of MWNT in a capillary glass tube and Raman spectra of DNA-encased MWNTs were obtained in aqueous solution using a glass cuvette.

The optical spectroscopy and Raman spectral properties of DNA-encased MWNTs were analyzed to determine to what extent DNA-encasement altered the physical properties of MWNTs. Shown in Figure 1a, absorption and scattering characteristics for aqueous solutions of DNA-encased MWNTs and PEG-solubilized MWNTs are compared. For both preparations, the expected $1/\lambda^4$ scattering dominates any specific absorption features of the DNA nucleobases (Murakami et al., 2005; Hughes et al., 2007). Optical absorbance spectroscopy in the 400 – 800 nm range did not reveal discrete absorbance bands for DNA-encased MWNTs that are characteristic of van Hove singularities (Carlson and Krauss, 2008). These absorbance bands also were not detected for MWNTs solubilized using PEG. Thus, the lack of detection probably arises from factors associated with the manufacture and purification of the MWNTs (Brennan et al., 2003; Pratap et al., 2005) rather than as a consequence of DNA complex formation with MWNTs.

Raman spectroscopy of the DNA-encased MWNTs revealed the presence of D, G, and G' bands that are characteristic of all graphitic materials (Fig. 2). The disorder-induced D band detected at 1351 cm^{-1} for the PEG-solubilized MWNTs was shifted to 1340 cm^{-1} for the DNA-encased MWNTs. Alterations in the D-band frequency and intensity have been attributed previously to charge transfer between DNA nucleobases and NTs (Bhatarrai et al., 2008). The D/G ratio was altered in the DNA-encased MWNTs relative to non-DNA-encased MWNTs. The radial breathing mode (RBM) was observed for both the DNA-encased MWNT sample as well as for non-DNA-encased MWNTs at ~475 cm-1 indicating the diameter or the innermost carbon nanotube in the MWNT is approximately 0.47 nm (Jinno et al., 2004). Analysis of AFM and SEM images revealed the diameter for the outermost carbon nanotube was > 40 nm (see following section) consistent with MWNTs consisting of multiple concentric layers, as expected.

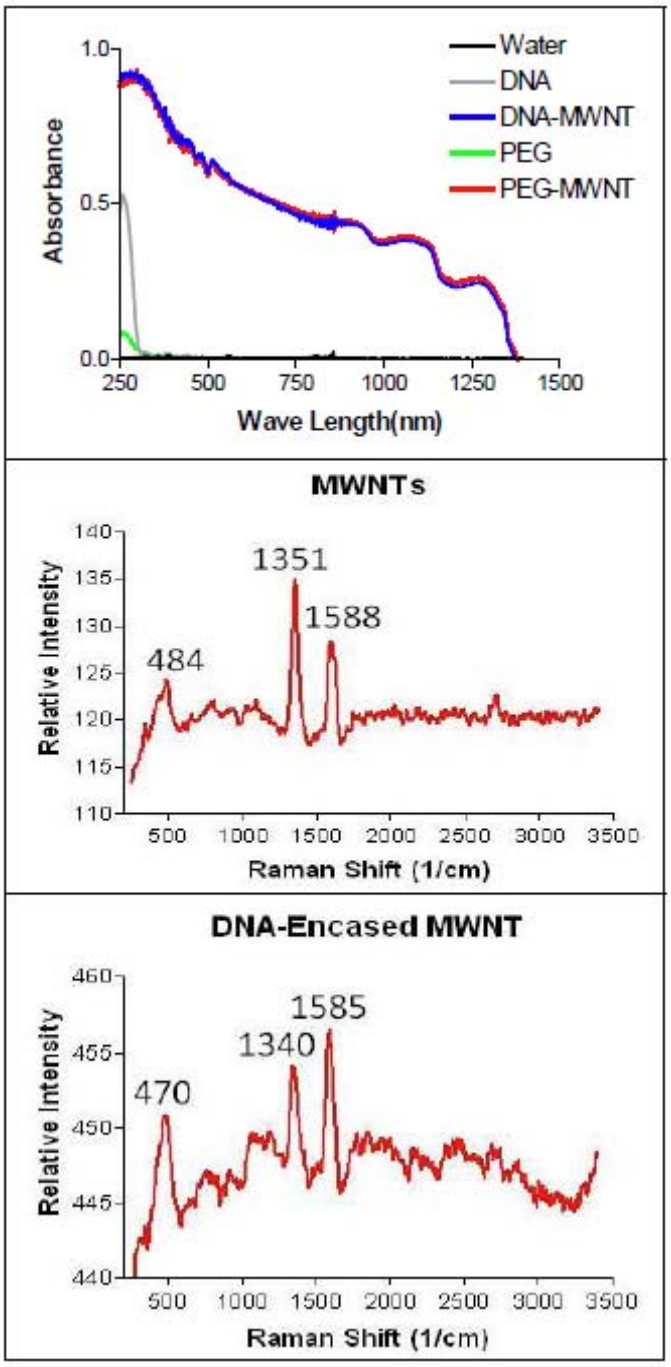

Figure 2: Raman Analysis

DNA coating of the nanotubes was qualitatively investigated with a fluorescence emission experiment. Single-stranded DNA (GT_{40}, with a fluorescent 6-FAM label at the 5'-end) was used to disperse and fluorescently label the nanotubes. After labeling, the nanotubes were extensively washed to remove free DNA. The sample was then irradiated with a laser (λ=488 nm), and the scattered light and fluorescent light were observed. The scattered light is blue (λ=488 nm), and can be observed without filter, while the emitted fluorescent light is green, and is observed with a 530 nm filter. The experiment was done on three different samples: 1) the FAM-labeled DNA (Fl-DNA), Fig. 3 A &B; DNA-MWCNT (0.1 mg/ml, vol- 1 ml), Fig. 3 C & D; and Fl-DNA-MWCNT (0.1

mg/ml, vol- 1 ml), Fig. 3 E & F. Fl-DNA-MWCNT and the Fl-DNA clearly showed green emission, while the DNA-MWCNT did not show any green emission (Fig. 3 C & D).

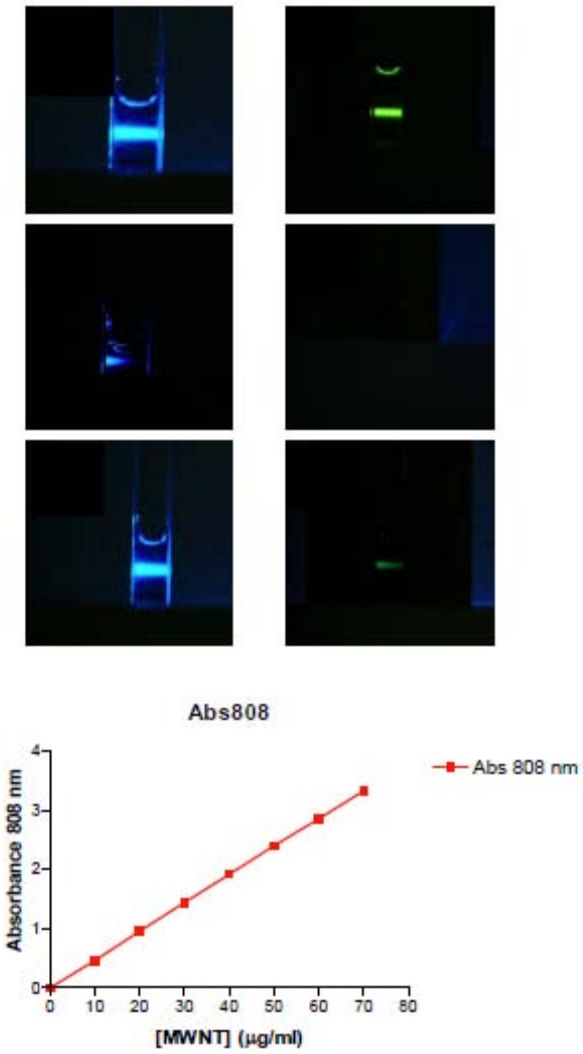

Figure 3: Fluorescence Spectroscopy of product

Task 1b.

In vitro Heating of DNA-encased MWNTs was tested. The heat emitted following near infrared (nIR) irradiation of aqueous solutions of DNA-encased MWNTs and MWNTs that had not been solubilized with DNA were evaluated by measuring the change in temperature for the aqueous solution using a digital thermometer. The 1 mL MWNT solutions were prepared at seven concentrations (1 – 100 µg/mL) and placed in sealed nIR-transparent glass cuvettes fitted with a micro temperature probe in the solution. Each sample was then irradiated at 1064 nm using a Photonix nIR laser system at a fixed power (2, 3, or 4 W/cm^2) for a fixed duration (30, 50, or 70 s). The initial temperature of each solution was recorded prior to irradiation and both the final temperature when laser power was turned off and the maximal temperature reached which occurred several seconds after turning laser power off were recorded.

Temperature was monitored using a digital continuous temperature monitoring system. The statistical significance of the measured temperature increases for samples of DNA-encased MWNTs and non-DNA encased MWNTs were analyzed using SAS v.

The extent of heating for aqueous solutions of DNA-encased MWNTs was evaluated to determine if encasing the MWNTs in DNA alters the utility of MWNTs as transducers of irradiated energy into heat. Aqueous solutions of DNA-encased MWNTs or MWNTs that had not been DNA-encased were irradiated at 1064 nm using a Photonics nIR laser system. Sample heating was evaluated for a range of MWNT concentrations (1 – 100 μg/mL) at three different power levels (2, 3, 4 W) and for times ranging from 25 – 70 s. Representative graphs from these experiments are included in Fig. 4.

For a given power level and time of irradiation, the DNA-encased MWNTs resulted in greater heating of the sample than that which occurred following irradiation of the same concentration of non-DNA-encased MWNTs (Fig. 4). Statistical analysis of the data revealed the heating of the DNA-encased MWNTs solutions was significantly greater than occurred for the non-DNA-encased MWNTs over a broad range of times, power levels, and concentrations. For example pairwise comparison of the mean values for DNA-encased MWNTs and non-DNA-encased MWNTs, both at a concentration of 10 μg/mL, for an irradiation time of 25 s, and irradiation power of 3 W revealed a significant difference ($p < 0.0001$). Significant differences were observed over a wide-range of concentrations as well as for the full range of power levels and irradiation times evaluated. Thus, encasing the MWNTs in DNA does not reduce the amount of heat generated and for most conditions evaluated, significantly increased the amount of heat generated following laser irradiation.

In some cases, the differential heating of DNA-encased MWNTs relative to non-DNA-encased MWNTs was substantial. For example, irradiation of a 10 μg/mL sample of DNA-encased MWNTs at 3 W for 70 sec resulted in a 10 °C temperature increase while irradiating the same concentration of non-DNA-encased MWNTs under comparable conditions resulted in a 6 °C rise. Modest temperature increases of 3 – 5 °C are sufficient to cause protein denaturation and subsequently cell death in living cells.

Importantly, the time-dependent increase in temperature for both DNA-encased MWNTs and non-DNA-encased MWNTs was approximately linear under all conditions evaluated. This finding indicates that DNA-encased MWNTs do not become saturated in any manner by continuous laser irradiation. Rather, the optical transitions responsible for transduction of laser light into thermal energy may be excited continuously over the second-minute timescale without any reduction in heat generation. Thus, irradiation of a lower concentration of DNA-encased MWNTs for a longer time period results in as much heat production as irradiation of a higher concentration for less time. These findings may be particularly significant under conditions where DNA-encased MWNTs are present at relatively low concentrations, as is likely to occur *in vivo* following i.v. administration.

In contrast to the linear–dependence of heat generation on time for a given concentration of DNA-encased MWNTs and power level of irradiation, the concentration-dependence of heat production for a given time and power level was non-linear at concentrations greater than approximately 10 μg/mL (Fig. 5 c,d). Further, the graphs indicate clear evidence of saturation (i.e. no further increase in temperature rise) at concentrations greater than 50 μg/mL. Interestingly, saturation was not evident for the non-DNA-encased MWNTs relative to the DNA-encased MWNTs (Fig 5 c,d). The physical basis for the differential concentration-dependent saturability of DNA-encased MWNTs relative to non-DNA-encased MWNTs is not known at present. The greater heat production for a given concentration of DNA-encased MWNTs relative to non-DNA-encased MWNTs is consistent with DNA-encasing reducing aggregation and with greater heat production per MWNT when in a non-aggregated state. The non-DNA-encased MWNTs continue to display proportionally greater heat production as concentration is increased indicating that aggregates of non-DNA-encased MWNTs are capable of transducing laser irradiation into heat. These data suggest that DNA-encasing MWNTs alters the physical properties of MWNT aggregates that form at higher MWNT concentrations.

The power dependence of heat generation for a given time and concentration was linear for both DNA-encased and non-DNA-encased MWNTs (Fig 5 e,f). Doubling of the laser power (from 2 to 4 W) approximately doubled the temperature increase for concentrations of DNA-encased MWNTs less than 25 μg/mL. Higher concentrations of DNA-encased MWNTs displayed identical power dependencies to one another. The power dependency for non-DNA-encased MWNT was also linear except for the highest concentration, 100 μg/mL, which consistently showed a greater temperature rise between 2 and 3 W compared to between 3 and 4 W. The slope of the power dependence for non-DNA-encased MWNTs was less steep than for DNA-encased MWNTs. Thus, for a given (non-saturating) concentration of MWNTs (e.g. 10 μg/mL), the temperature rise associated with the DNA-encased MWNTs was greater than for the non-DNA-encased MWNTs at both low and high power, however the differential was enhanced at higher power levels (Fig 5 e,f).

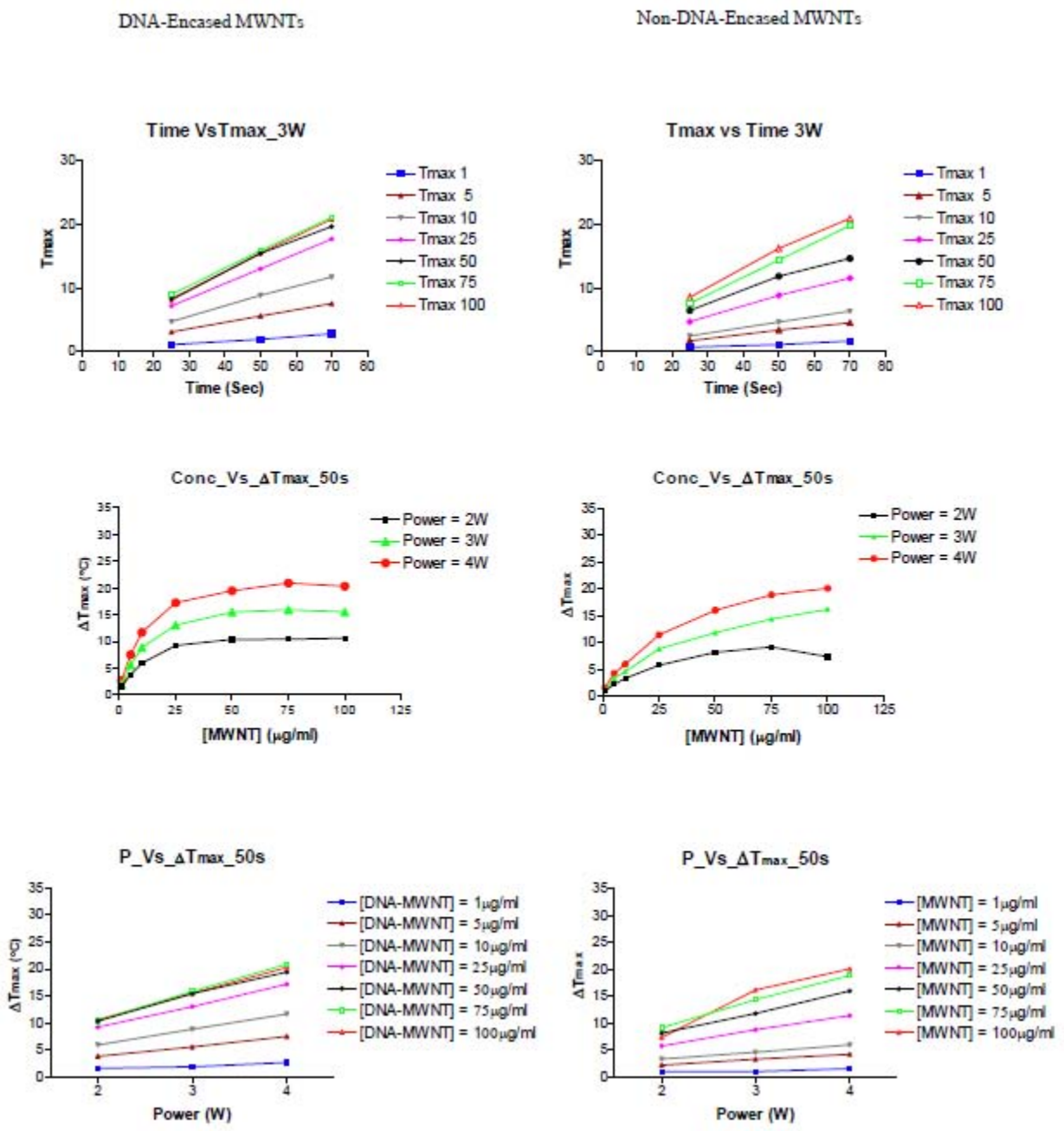

Figure 4: in vitro heating

Cell death in **MCF7 and MDA MB 231 as well as SK-Br-3 and BT474** cancer cell lines was monitored using fluorescently tagged cells. Though not shown here, complete cell death was achieved in culture when culture temperatures exceeded 52^{o}C as we have previously reported. These correlated exactly with the data in figure 4.

***Task 2: Targeting and ablation of breast cancer cells in cell culture and mouse models, with the Herceptin- CNWs*:**

a. **The interaction of the Herceptin-CNW conjugate will be tested in the immunoblotting and immunofluorescence experiments. We will employ HER-2 negative breast cancer cells (MCF-7 and MDA MB 231) and HER-2 positive cells (SK-Br-3 and BT474), and a Herceptin resistant BT474 cell line. (Month 6 – 8)**
b. **We will demonstrate that the conjugated nanotubes photothermally-ablate Herceptin positive breast cancer cells orthotopically implanted in athymic nude mice. (Month 9 – 10)**
c. **We will determine the optimized concentration of the conjugate for given depths within the mice. (Month 11-12)**

Task2a

The N-MWNT conjugates with herceptin mentioned above were put into solution with HER-2 negative breast cancer cells (MCF-7 and MDA MB 231) and HER-2 positive cells (SK-Br-3 and BT474), and a Herceptin resistant BT474 cell lines. Using different concentrations and different wait times the well mixed cell-nanotube solutions were studied using light scattering to determine the level of binding and aggregation in the solutions. This was taken as an indication of specific binding between the cells and the nanotube conjugates. We determined that there was no difference between HER2 positive and HER2 negative cells indicating that the HER 2 was not being bound in the experiment. This is not surprising since the herceptin was previously determined to have become denatured due to the proximity of the nanotube. Upon further microscopic examination, we found no specific binding between the conjugated nanotubes and the HER 2 positive cells. Direct injection into MCF7 tumor xenographs were successful in removal of the tumors upon heating as reported previously and now in literature. However no specific targeting was achieved.

However the DNA (aptamer) encased nanotubes COULD be used in targeting. To test this a model was prepared to which the aptamer could target.

Task2b

All animal experiments were performed under the protocol approved by animal care committee of the Wake Forest University Baptist Medical Center. Tumor xenografts were generated by sub-cutaneous injection of 3 x 10^6 PC3 cells suspended in 100 µl of 1:1 PBS:Matrigel in both flanks of 12 male nude mice. Mice were used for experimental procedures two weeks following inoculation with tumor cells, after tumor size had reached 200 – 250 mm^3. Each of the 12 mice were treated with 100 µL of 500 µg/mL solution of DNA-encased MWNTs injected into the right-flank tumor and 100µl of sterile water injected into the left-flank tumor. After 1.5 h, the tumors on both flanks of 8 mice were irradiated using a NIR quasi-CW-YAG laser beam pulses with 5 sec on & 3 sec off for total exposure time 70 sec at the power level of 2.5W/cm^2. The remaining four mice were treated identically but were not exposed to the laser. The tumor sizes were measured by a caliper every third day and photographs of tumors were taken once per week. The tumor volumes were calculated using the formula x * y^2 * pi/6 (where x and y are the long and short diameters of the tumor, respectively).

The tumors were analyzed as four independent groups: 1) No laser, no MWNT; 2) Laser, no MWNT; 3) No laser, MWNT; 4) Laser, MWNT. The statistical significance of tumor volume measurements among the four groups were measured using SAS v.

The selective eradication of tumor tissue as a result of localized hyperthermia is an important objective in cancer treatment. In this study, DNA-encased MWNTs (100 μL of a 500 μg/mL solution) were injected directly into sub-cutaneous human tumor xenografts formed from PC3 (human prostate cancer) cells. Tumors were formed bilaterally, and treatment was initiated when tumor volumes were approximately 225 mm^3. There was no difference in tumor volumes among the four treatment groups at baseline: 1) MWNT+Laser; 2) Laser-only; 3) MWNT-only; 4) no treatment. The treatment groups consisted of both left and right flank tumors from a total of 12 mice.

For the MWNT+ laser treatment group, the left flank tumor for each of eight mice was selectively irradiated at 1064 nm for 70 s with a Photonic nIR laser system one hour following intratumoral injection of the DNA-encased MWNT solution. The location of the DNA-encased MWNTs following intratumoral injection was readily evident by the bluish-grey color at the site of injection. For the laser-only group, the eight animals that were selectively irradiated on the left flank tumor for the MWNT+laser group were also selectively irradiated on the right flank tumor. The right-flank tumor, however, received an intratumoral injection of saline and not DNA-encased MWNTs. The left flank tumor for four other mice was injected with DNA-encased MWNTs, but the left-flank tumors for these mice were not irradiated with a laser (MWNT-only group). The right flank tumor for these four mice received neither laser irradiation nor MWNT injection (no treatment group). The results are displayed in Fig. 6. Of the four treatment groups (MWNT + Laser, MWNT-only, laser-only, no treatment) only those tumors that received both an intratumoral injection of DNA-encased MWNTs and were subject to laser irradiation underwent a regression in tumor size. The tumors in the MWNT + laser group were all completely eradicated by day 6 following the single treatment (Figure 6).

Statistical analysis of the tumor volume data revealed that the mean tumor size for the MWNT+laser group diverged from the mean values for the other three groups (laser-only; MWNT-only; no treatment) beginning on day 6 and persisting until the end of the study. For example, comparison of the MWNT+laser to MWNT-only showed a statistical significance beginning on day 6 ($p = 0.0109$) that increased in significance at later time points ($p < 0.0001$ at day 24 and day 30). The MWNT+laser group showed similar statistical significance relative to the laser-only group ($p < 0.0001$ beginning on day 10 and persisting through the study) and the no treatment group ($p < 0.0001$ beginning on day 17). The three control groups (MWNT-only, laser only, no treatment) did not show a statistically significant difference in tumor volume at any time during the study (MWNT-only vs no treatment $p = 0.6094$ at day 30). Thus, the effectiveness of treatment requires both the presence of MWNTs and laser irradiation.

Those tumors that were both injected with DNA-encased MWNTs and irradiated with the nIR laser were completely eradicated by treatment. Tumors that received an MWNT-injection but were not lased did not display any different growth characteristics relative to untreated tumors. Similarly, tumors that were lased but that were not injected with MWNTs displayed growth characteristics indistinguishable from control tumors.

Tumors that received both an intratumoral injection of DNA-encased MWNTs and irradiation with a nIR laser displayed a minor surface burn to the skin. An antibiotic ointment was applied to the burned area and a scab formed over the burn. The scab fell off each of the tumors within 2-3 days of the lasing procedure and the area that had been occupied by the tumor completely healed over for all eight of the animals treated. In no case, was there any evidence of tumor re-growth nor was there any evidence of long-term damage to skin. The results indicate that DNA-encased MWNTs are useful for the selective thermal eradication of malignant or hyperproliferative tissue and that this can be accomplished without any long-term damage to adjacent normal tissue.

A

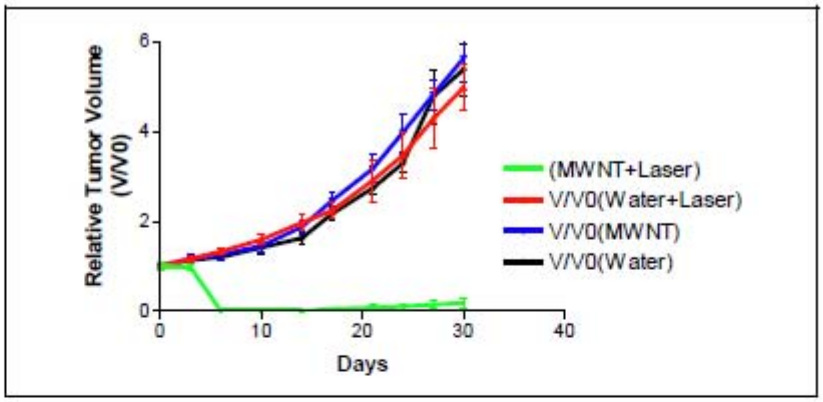

B

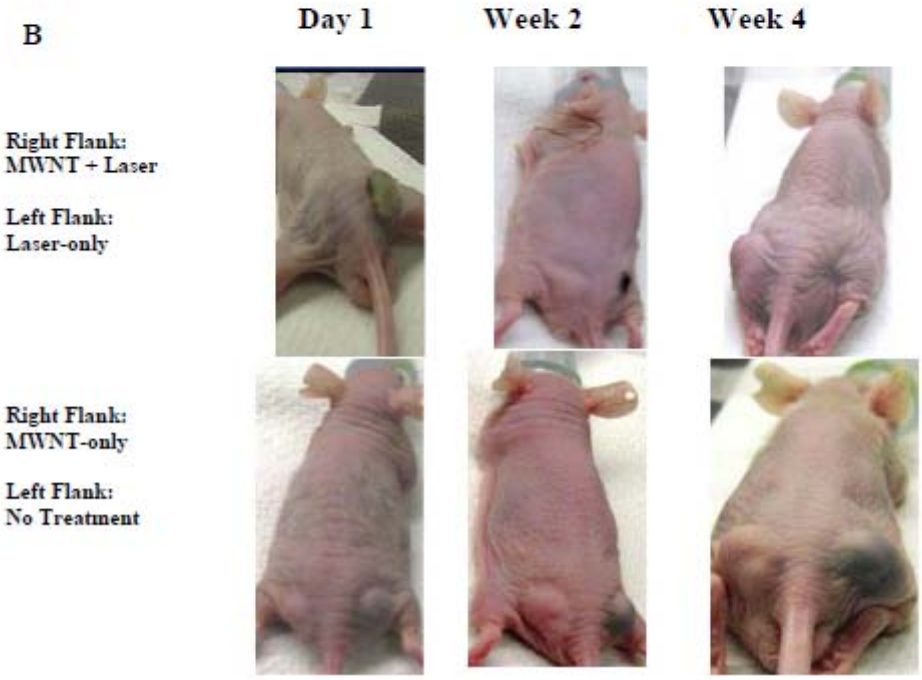

Figure 5: Laser ablation of PC3 xenographs

Conclusions:

During this experiment we discovered that herceptin conjugated N-doped MWNTs could not target HER2 positive breast cancer lines. This was determined to be due to denatured herceptin. In order to provide some idea of the concept and its validity once a targeting meaty was successfully attached we were forced to switch to a PC3 mouse model using aptamers as the targeting method. The negative results of the herceptin conjugation was thusly turned into a positive demonstration of targeting using nanotubes conjugated with a DNA fragment.

There is considerable interest in the use of nanotechnology for cancer diagnosis and treatment with projected applications in drug delivery, imaging (de la Zerda et al., 2008), and other areas. The present study has demonstrated that DNA-encased MWNTs that are soluble in aqueous solution (Zheng et al. 2002; Kam et al., 2005; Vogel et al., 2007) display thermal heating properties that are comparable to, and in several aspects superior to those displayed by non-derivatized MWNTs. Previous studies have demonstrated that SWNTs that have been solubilized by either DNA-encasement or with PEG may be excited upon irradiation with nIR to release heat sufficient for lethality towards cancer cells in tissue culture (Kam et al., 2005). In the present study, we have demonstrated that the conversion of nIR irradiation to heat by DNA-encased MWNTs is linear with respect to both power and time indicating that control of these parameters can be exercised to provide the desired selectivity of cell kill in vivo. Further, we have demonstrated that DNA-encased MWNTs can be used for the selective eradication of malignant tissue *in vivo*.

References:

Brennan, M. E., Coleman, J. N., Drury, A., Lahr, B., Kobayashi, T., and Blau, W. J. (2003). Nonlinear photoluminescence from van Hove singularities in multiwalled carbon nanotubes. Opt Lett *28*, 266-268.

Carlson, L. J., and Krauss, T. D. (2008). Photophysics of individual single-walled carbon nanotubes. Acc Chem Res *41*, 235-243.

Chakravarty, P., Marches, R., Zimmerman, N. S., Swafford, A. D., Bajaj, P., Musselman, I. H., Pantano, P., Draper, R. K., and Vitetta, E. S. (2008). Thermal ablation of tumor cells with antibody-functionalized single-walled carbon nanotubes. Proc Natl Acad Sci U S A *105*, 8697-8702.

Deng, Y., Deng, C., Yang, D., Wang, C., Fu, S., and Zhang, X. (2005). Preparation, characterization and application of magnetic silica nanoparticle functionalized multi-walled carbon nanotubes. Chem Commun (Camb), 5548-5550.

Dorin Boldor*†, N. M. G., William T. Monroe†, Jason H. Palmer†, Zhongrui Li‡ and Alexandru S. Biris‡ (2008). Temperature Measurement of Carbon Nanotubes Using Infrared Thermography Chemistry of Materials *20*, 4011-4016.

Fagan, J. A., Simpson, J. R., Bauer, B. J., Lacerda, S. H., Becker, M. L., Chun, J., Migler, K. B., Walker, A. R., and Hobbie, E. K. (2007). Length-dependent optical effects in single-wall carbon nanotubes. J Am Chem Soc *129*, 10607-10612.

Gannon, C. J., Cherukuri, P., Yakobson, B. I., Cognet, L., Kanzius, J. S., Kittrell, C.,

Weisman, R. B., Pasquali, M., Schmidt, H. K., Smalley, R. E., and Curley, S. A. (2007). Carbon nanotube-enhanced thermal destruction of cancer cells in a noninvasive radiofrequency field. Cancer *110*, 2654-2665.

Gannon, C. J., Patra, C. R., Bhattacharya, R., Mukherjee, P., and Curley, S. A. (2008). Intracellular gold nanoparticles enhance non-invasive radiofrequency thermal destruction of human gastrointestinal cancer cells. J Nanobiotechnology *6*, 2.

He, X., Wolkers, W. F., Crowe, J. H., Swanlund, D. J., and Bischof, J. C. (2004). In situ thermal denaturation of proteins in dunning AT-1 prostate cancer cells: implication for hyperthermic cell injury. Ann Biomed Eng *32*, 1384-1398.
Helen Cathcart, S. Q., Valeria Nicolosi, John M. Kelly, Werner J. Blau, and Jonathan N. Coleman (2007). Spontaneous Debundling of Single-Walled Carbon Nanotubes in DNA-Based Dispersions Journal of Physical Chemistry C *111*, 66-74.

Huang, X., Jain, P. K., El-Sayed, I. H., and El-Sayed, M. A. (2006). Determination of the minimum temperature required for selective photothermal destruction of cancer cells with the use of immunotargeted gold nanoparticles. Photochem Photobiol *82*, 412-417.

Hughes, M. E., Brandin, E., and Golovchenko, J. A. (2007). Optical absorption of DNA-carbon nanotube structures. Nano Lett *7*, 1191-1194.

Jie Han, M. P. A., and R. L. Jaffe, J. Kong and H. Dai (1998). Observation and modeling of single-wall carbon nanotube bend junctions PHYSICAL REVIEW B *57*, 14 983-914 989.

Jindal, G., Friedman, M., Locklin, J., and Wood, B. J. (2006). Palliative radiofrequency ablation for recurrent prostate cancer. Cardiovasc Intervent Radiol *29*, 482-485.

Johnson, R. R., Johnson, A. T., and Klein, M. L. (2008). Probing the structure of DNA-carbon nanotube hybrids with molecular dynamics. Nano Lett *8*, 69-75.

Kam NW, O. C. M., Wisdom JA, Dai H (2005). Carbon nanotubes as multifunctional biological transporters and near-infrared agents for selective cancer cell destruction. PNAS *102* 11600-11605.

Kazuyuki, O. T. K. T. H. R. T. (2006). Electrically triggered insertion of single-stranded DNA into single-walled carbon nanotubes Chemical physics letters *417*, 288-292.

KIM, S. R. B. A. S. R. B. K. C. B. N. P. H. H. H. K. Y. H. Y. (2008). Carbon nanotube-hydroxyapatite nanocomposite for DNA complexation Materials science & engineering C Biomimetic and supramolecular systems *28*, 64-69.

Lencioni, R., Crocetti, L., Cioni, R., Suh, R., Glenn, D., Regge, D., Helmberger, T., Gillams, A. R., Frilling, A., Ambrogi, M., *et al.* (2008). Response to radiofrequency ablation of pulmonary tumours: a prospective, intention-to-treat, multicentre clinical trial (the RAPTURE study). Lancet Oncol *9*, 621-628.

Levy-Nissenbaum, E., Radovic-Moreno, A. F., Wang, A. Z., Langer, R., and Farokhzad, O. C. (2008). Nanotechnology and aptamers: applications in drug delivery. Trends Biotechnol *26*, 442-449.

Liang, P., and Wang, Y. (2007). Microwave ablation of hepatocellular carcinoma. Oncology *72 Suppl 1*, 124-131.

Liu, Z., Chen, K., Davis, C., Sherlock, S., Cao, Q., Chen, X., and Dai, H. (2008). Drug delivery with carbon nanotubes for in vivo cancer treatment. Cancer Res *68*, 6652-6660.

Liu, Z., Davis, C., Cai, W., He, L., Chen, X., and Dai, H. (2008). Circulation and long-term fate of functionalized, biocompatible single-walled carbon nanotubes in mice probed by Raman spectroscopy. Proc Natl Acad Sci U S A *105*, 1410-1415.

Murakami, Y., Einarsson, E., Edamura, T., and Maruyama, S. (2005). Polarization dependence of the optical absorption of single-walled carbon nanotubes. Phys Rev Lett *94*, 087402.

Pratap, A. S., A.2; Singh, A.2; Pal, S.2; Tyagi, R.2; Dawar, A.2; Chaturvedi, P.3; Lamba, S.3; Bal, M.3; Harsh3 (2005). Linear and non-linear optical transmission from multi-walled carbon nanotubes
Journal of Materials Science *40*, 4185-4188(4184).

Schipper, M. L., Nakayama-Ratchford, N., Davis, C. R., Kam, N. W., Chu, P., Liu, Z., Sun, X., Dai, H., and Gambhir, S. S. (2008). A pilot toxicology study of single-walled carbon nanotubes in a small sample of mice. Nat Nanotechnol *3*, 216-221.
Shvartzman-Cohen, R., Florent, M., Goldfarb, D., Szleifer, I., and Yerushalmi-Rozen, R. (2008). Aggregation and self-assembly of amphiphilic block copolymers in aqueous dispersions of carbon nanotubes. Langmuir *24*, 4625-4632.

Torti, S. V., Byrne, F., Whelan, O., Levi, N., Ucer, B., Schmid, M., Torti, F. M., Akman, S., Liu, J., Ajayan, P. M., *et al.* (2007). Thermal ablation therapeutics based on CN(x) multi-walled nanotubes. Int J Nanomedicine *2*, 707-714.

Vogel, S. R., Kappes, M. M., Hennrich, F., and Richert, C. (2007). An unexpected new optimum in the structure space of DNA solubilizing single-walled carbon nanotubes. Chemistry *13*, 1815-1820.

Welsher, K., Liu, Z., Daranciang, D., and Dai, H. (2008). Selective probing and imaging of cells with single walled carbon nanotubes as near-infrared fluorescent molecules. Nano Lett *8*, 586-590.

Y, J. M. B. S. A. (2004). Multiwalled carbon nanotubes produced by direct current arc discharge in hydrogen gas. Chemical physics letters *398*, 256-259.

Yang, R., Jin, J., Chen, Y., Shao, N., Kang, H., Xiao, Z., Tang, Z., Wu, Y., Zhu, Z., and Tan, W. (2008). Carbon nanotube-quenched fluorescent oligonucleotides: probes that fluoresce upon hybridization. J Am Chem Soc *130*, 8351-8358.

Zheng, M., Jagota, A., Semke, E. D., Diner, B. A., McLean, R. S., Lustig, S. R., Richardson, R. E., and Tassi, N. G. (2003). DNA-assisted dispersion and separation of carbon nanotubes. Nat Mater *2*, 338-342.

Zheng, M., Jagota, A., Strano, M. S., Santos, A. P., Barone, P., Chou, S. G., Diner, B. A., Dresselhaus, M. S., McLean, R. S., Onoa, G. B., *et al.* (2003). Structure-based carbon nanotube sorting by sequence-dependent DNA assembly. Science *302*, 1545-1548.